Unsupervised Clustering for Millimeter-Wave Channel Propagation Modeling

Jian Wang[1], Camillo Gentile[1], Jelena Senic[2], Ruoyu Sun[2], Peter B. Papazian[2], Chiehping Lai[1]

[1]Wireless Networks Division, National Institute of Standards and Technology, Gaithersburg, MD, USA
[2]RF Technology Division, National Institute of Standards and Technology, Boulder, CO, USA
e-mail: {jian.wang, camillo.gentile, jelena.senic, ruoyu.sun, peter.papazian, chiehping.lai}@nist.gov

***Abstract*—To date, we have designed and assembled millimeter-wave channel sounders at 60 GHz and 83 GHz. They can estimate the angle-of-departure and angle-of-arrival of channel multipath components as well as their delay and Doppler frequency shift. In addition, due to the fast acquisition time and because the receiver is mounted on a mobile robot, the systems can collect measurements for hundreds of different transmitter-receiver configurations in just minutes. It follows that channel-model reduction, including the multipath-component clustering process, must be reliable, consistent, and unsupervised. In this paper, we describe a simple clustering process tailored to the properties of millimeter-wave channels that fully exploits the multi-dimensionality of the extracted multipath components and requires only a few tunable parameters. Through extensive experimentation, we have verified that the process is robust and delivers consistent results across five different environments and across both frequency bands investigated. Illustrative examples are provided.**

Index Terms— 5G; double-directional channel; mmWave.

I. Introduction

The inherent drawback of millimeter-wave (mmWave) bands compared to sub-6-GHz bands is greater path loss due to free-space[1], oxygen-absorption, and/or penetration losses. To compensate the link budget, extremely high-gain – in turn extremely narrow-beam – antennas will be employed. Given their limited beamwidth, the antennas must be electronically steered in azimuth and elevation along the angle-of-departure (AoD) and angle-of-arrival (AoA) of any viable propagation paths between the respective transmitter (TX) and receiver (RX) to provide omnidirectional fields of view. Hence from a channel-modeling perspective, it is fundamental to understand how many paths are available in an environment and their distribution in both delay and 3D double-directional angle (azimuth AoD, elevation AoD, azimuth AoA, elevation AoA).

Diffraction at mmWave frequencies has been demonstrated to be significantly weaker than at sub-6-GHz [1]. The absence of diffraction renders the channel "sparse," meaning that only a few dominant multipath components (MPCs) will be detected. The strongest will be the direct path (in line-of-sight (LOS) conditions) while the others will originate from specular reflections off ambient objects. Each specular reflection gives rise to scattering of the incident wave into a dominant specular multipath component and weaker diffuse components surrounding in the multi-dimensional delay-angle space; altogether they form a *cluster*. The dominant paths can be exploited to send multiple data streams between the TX and RX. In other words, the number of clusters will determine the maximum number of independent streams that can be sent in one polarization[2].

Whether the clusters are distributed randomly in the delay-angle space (e.g. WINNER II [3], COST 2100 [4] 5GCMSIG [5]) or follow a deterministic map-based distribution (e.g. METIS2020 [6], MiWEBA [7], mmMAGIC [8]), a fundamental process in reducing channel models is clustering the MPCs extracted from measurements. Besides their distribution in space, also important are the delay- and angle-dispersion characteristics of the clusters, i.e. their shape. When clusters overlap, separating them is a challenge. There are two reasons why the challenge is diminished in mmWave systems compared to legacy systems: 1. the channel is sparse, hence there are less components a priori; 2. 5G systems will fully exploit the multi-dimensionality of the channel – for proper radio and network design, the path loss of the extracted MPCs should be polarization-dependent (VV, VH, HV, HH) and indexed according to delay, 3D double-directional angle, and Doppler frequency shift – hence cluster overlap in all six dimensions is less likely.

To date, we have designed and assembled mmWave channel sounders at 60 GHz [9] and at 83 GHz [10]; the latter features a three-dimensional switched array at the RX for AoA discrimination in both azimuth and elevation while the former features an array at the TX as well for AoD discrimination. Besides high delay resolution (up to 0.5 ns), the systems are capable of estimating Doppler shift. In addition, due to the fast acquisition time and because the RX is mounted on a mobile robot, the systems can collect channel measurements for hundreds of different TX-RX configurations in just minutes. It follows that model reduction, including the MPC clustering process, must be reliable, consistent, and unsupervised.

In this paper, we describe a simple clustering process tailored to the properties of both mmWave channels and 5G systems that accepts only a few tunable parameters. Through extensive measurements, we verified the process to be robust and deliver consistent results across five different environments (lecture room, lobby, hallway, basement, and data center) in LOS and non-LOS conditions and across both frequency bands. The remainder of this paper is organized as follows. In Section II, we present our clustering process. In Section III, we show some illustrative examples. Finally, we draw some important conclusions in Section IV.

[1]Assuming a frequency-dependent aperture size, not a fixed physical antenna size.

[2]Dually polarized streams are provisioned for mmWave systems [2].

978-1-5090-5935-5/17/$31.00 ©2017 IEEE

II. CLUSTERING PROCESS

In this section, we describe the process through which the multipath components extracted from a channel measurement are clustered. Before the process begins, we check whether the TX-RX configuration lies in LOS conditions; if so, the direct path – the strongest of all MPCs – is easily detected and removed[3]. As there is no scattering associated with it, nor are there diffuse components surrounding it. As such, the clustering is only applied to the remaining components.

The components to be clustered are indexed through i. Each is characterized by path gain[4] PG_i (in dB) in the space $\boldsymbol{x}_i = (\tau_i, \theta_i^{A,AoD}, \theta_i^{E,AoD}, \theta_i^{A,AoA}, \theta_i^{E,AoA}, \nu_i)$, where τ denotes delay, θ the azimuth (A) or elevation (E) AoD or AoA, and ν the Doppler frequency shift. Fig. 1(a) displays an example of MPCs extracted from a measurement in a data center with our 60 GHz system. The floorplan of the environment and the TX-RX configuration are shown in Fig. 1(b). Because each dimension j will have a different range, the space is normalized as

$$\hat{x}_i^j = \frac{x_i^j - \min_i x_i^j}{\max_i x_i^j - \min_i x_i^j}$$

so that every $\hat{x}_i^j$ falls within the range [0,1]. The clustering is then carried out in the normalized space.

Often clusters from a single acquisition contained too few components, prohibiting sufficient statistical characterization of the shape. As such, for each TX-RX configuration, in reality MPCs from 8 acquisitions were aggregated while the RX was moving on the mobile robot; since acquisitions were at least a wavelength apart, the scattering between them is known to be independent. Fig. 2 shows a cluster identified in the data center indexed in the delay dimension only. Each symbol represents a different acquisition. Note that the specular components (blue) are significantly stronger than the diffuse components (green).

The remainder of this section is partitioned into three subsections, each describing a sequential step of the clustering process:

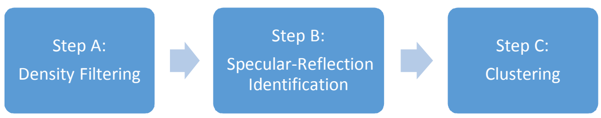

A. Density Filtering

The first step of the clustering process is to filter out any spurious paths, typically originating from weak diffraction or small ambient objects. To this end, we apply the DBSCAN (Density-Based Spatial Clustering of Applications with Noise) algorithm [11]. In the algorithm, each MPC is scanned to determine whether it is surrounded by at least N_m paths (including itself) within some radius ε, using the Euclidean distance metric in the space. If so,

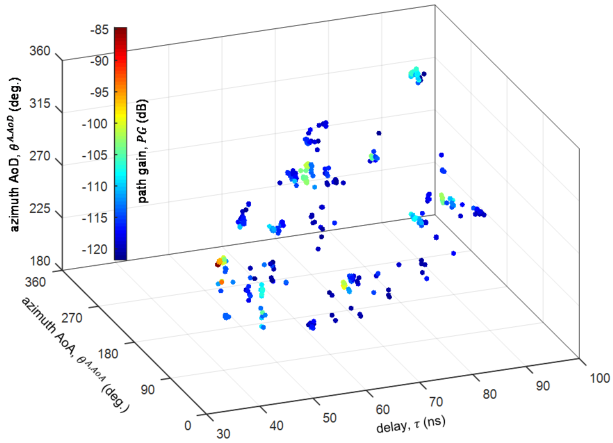

Fig. 1(a). Multipath components extracted from a measurement in a data center with our 60 GHz system. Each component is indexed in delay, azimuth AoD, and azimuth AoA (elevation AoD, elevation AoA, and Doppler shift are omitted) and is color-coded against the path-gain legend.

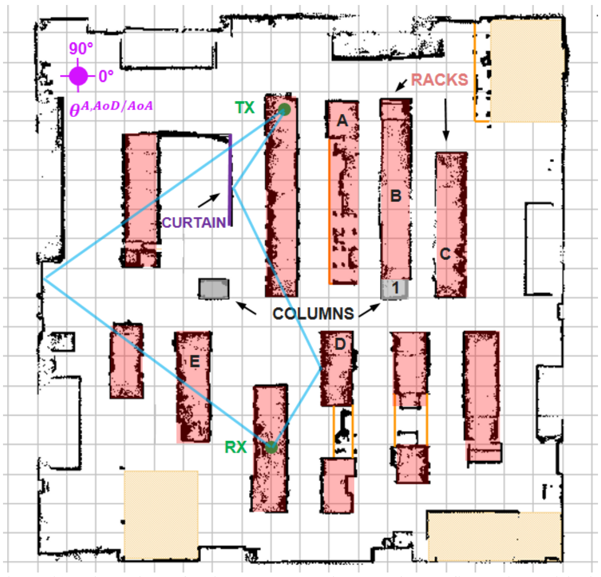

Fig. 1(b). Floorplan of a data center and example configuration with the TX and RX on top of racks. Reflectors that generated the detected multipath components in the channel measurement are labeled. Shown in cyan are example first- and second-order reflections from ambient objects.

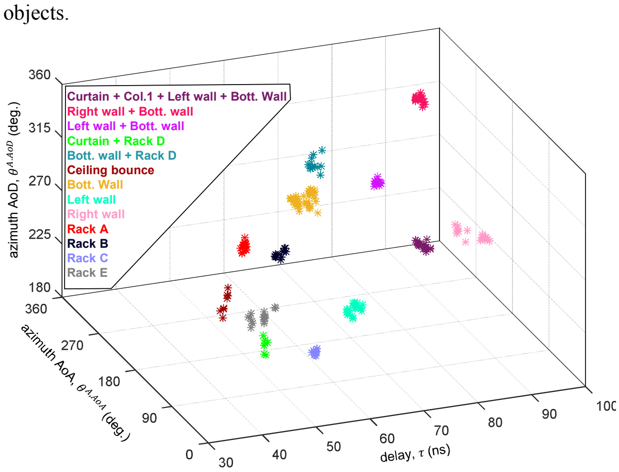

Fig. 1(c). Clustering of multipath components in Fig. 1(a). Each cluster is displayed as a different color and is labeled in reference to the reflector(s) in Fig. 1(b) that generated it.

[3]In non-LOS conditions, the direct path is assumed to go undetected as penetration loss at mmWave frequencies is very high.

[4]In our measurements, we only had VV polarization; but if multiple polarizations are available, they could be exploited as separate dimensions for enhanced discrimination.

the MPC is designated as a *core point*. Then all neighbors (within the same radius ε) of a core point (including the core point itself) are designated as *reachable* and so kept; otherwise they are deemed outliers and consequently discarded. This step yields multiple *regions*, each a collection of mutually reachable MPCs.

In our experiments, we set $\varepsilon = 0.04$ fixed and N_m to vary between 3 and 8 as

$$N_m = \left\lceil \frac{8}{3} \cdot 3^{\widehat{PG}_i} \right\rceil,$$

$$\widehat{PG}_i = \frac{PG_i - \min_i PG_i}{\max_i PG_i - \min_i PG_i}.$$

Hence the condition on the number of neighbors is relaxed with lower path gain. While these parameters can be tuned through visual inspection on a sample set of measurements, we found them to be robust and as such were maintained constant across the five environments and two center frequencies tested.

B. Specular-Reflection Identification

A defining feature of clusters at mmWave frequencies is that each one contains a single specular component marked by a peak in path gain. It may occur that multiple specular components fall within a region delineated in Step A. This will occur especially if the dimensionality of the MPC space is reduced due to the limitations of the measurement system. What happens is that the MPCs are projected into a lower dimensional space, increasing chances of cluster overlap. In order to resolve separate clusters, we identify peaks within a region under the premise that each peak is linked to a specular component.

As can be observed from the example in Fig. 2, local peaks will arise due to random fluctuation of the path gain in delay. Although the delay dimension only is shown, it holds true for the other dimensions as well. As a means to isolate the global peaks in each region, we filter the path gain in the multi-dimensional space to smooth out the local peaks. First we interpolate the path gain between the MPCs through the LOWESS (Locally Weighted Scatterplot Smoothing) algorithm with robust bisquare weights [12]. This algorithm is used in regression analysis to create a continuous surface while attenuating the effect of outliers. Then we apply a Gaussian filter to average over any residual local peaks. The standard deviation of the filter is set to $\sigma = \Delta x^{\max}/12$, where $\Delta x^{\max}$ is the maximum length of the region over all dimensions. Finally, we isolate the global peaks by comparing them to their neighboring values in the smoothed space.

C. Clustering

The clustering step is initialized by pinning the clusterheads to the coordinates of the global peaks identified over all regions in Step B; hence the number of clusters corresponds to the number of global peaks. We then apply the K-Power Means Clustering algorithm [13]. In one iteration, individual MPCs are assigned to the clusterhead for which the Euclidean distance is minimum. Once the MPCs have been all assigned, the clusterhead is recomputed as the weighted centroid of the MPCs assigned to the cluster; the path gain is the weight. The iterations continue until convergence.

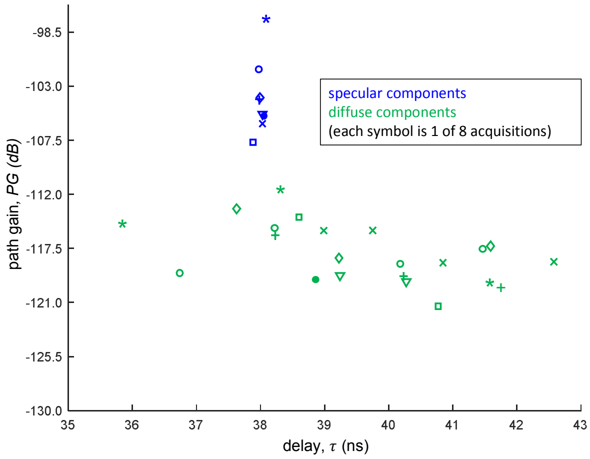

Fig. 2. Multipath components of an example cluster aggregated over eight small-scale acquisitions (each one shown with a different symbol).

III. Experimental Results

Fig. 1(c) shows the clustering results for the example measurement in the data center. Each cluster is marked with a different color. The results were validated through an exercise parallel to the measurements: the specular reflections were raytraced for the TX-RX configuration given the floorplan of the environment. Then the delay, AoD, and AoA of the raytraced paths were compared with the same properties of the specular reflections identified from the measurements and paired accordingly. The purpose was to discern the number and type of reflectors on each path from the paired raytraced path (for which this information was furnished). In Fig. 1(c), the reflectors on each of the 13 paths (one for each cluster) were labeled in reference to Fig. 1(b). Fig. 1(b) also displays paired raytraced paths for two of the 13 (the other 11 were omitted to avoid clutter). Good agreement between the locations of the reflectors in the floorplan and their delay-angle properties was witnessed, validating the mmWave cluster model.

To further substantiate the effectiveness of our clustering process, we illustrate another example with our 83 GHz system in a lecture room. Fig. 3(a) shows the MPCs extracted from the measurement for the TX-RX configuration in Fig. 3(b). Note that since there is no TX array for this system – only a single element – we could not estimate AoD. Finally, Fig. 3(c) shows the clustering results: 10 clusters are shown and each cluster is traced back to the main reflectors in Fig. 3(b).

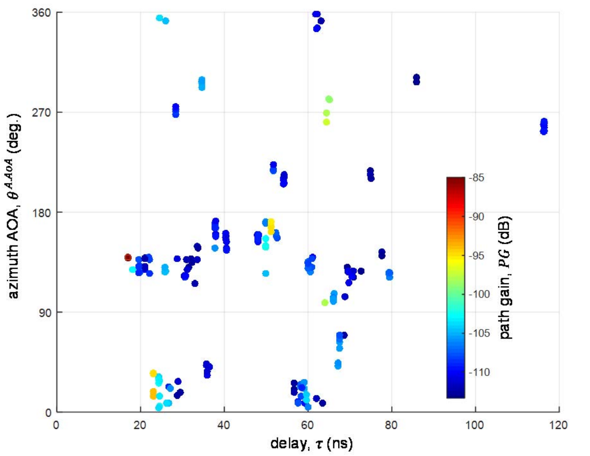

Fig. 3(a). Multipath components extracted from a measurement in a lecture room with our 83 GHz channel sounder. Each component is indexed in delay and azimuth AoA (elevation AoA and Doppler shift are omitted) and is color-coded against the path-gain legend.

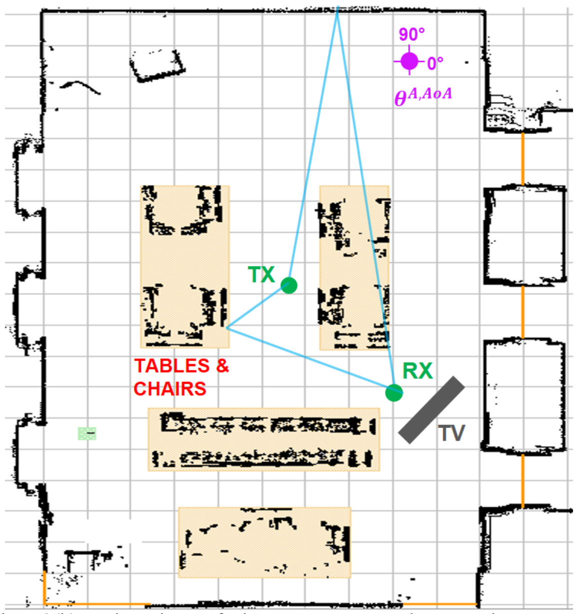

Fig. 3(b). Floorplan of lecture room and example TX-RX configuration. Reflectors that generated the detected multipath components in the channel measurement are labeled. Reflections off the Top wall and the Tables & Chairs are shown in cyan.

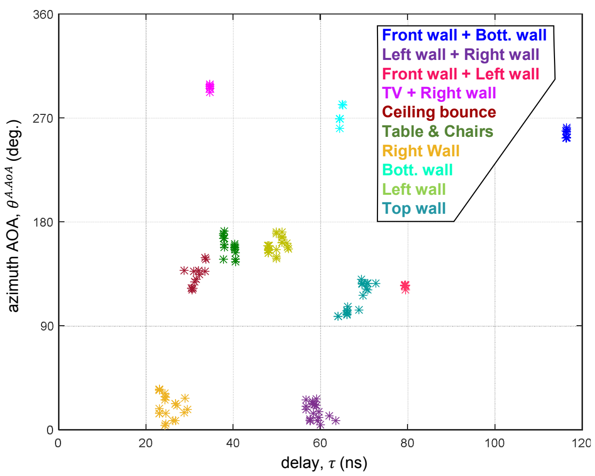

Fig. 3(c). Clustering of multipath components in Fig. 3(a). Each cluster is displayed as a different color and is labeled in reference to the reflector(s) in Fig. 3(b) that generated it.

IV. Conclusions

In this paper, we describe a clustering process for multipath components extracted from measurements with millimeter-wave channel sounders at 60 GHz and 83 GHz. The process contains few tunable parameters which are verified to be robust against measurements taken in five different environments and across the two frequency bands. While a total of six MPC dimensions are viable for clustering, the key findings of our analysis are:

1. The azimuth dimension is much more distinct than elevation because, given typical TX, RX, and ceiling heights, ground and ceiling bounces will impinge at shallow elevation angles with little variability amongst them. Elevation angle is most useful to discriminate ground from ceiling bounces at short distances (less than 5 m or so).
2. AoD and AoA are both critically important because two paths will often arrive (depart) at similar angles but with different departure (arrival) angles. They are otherwise inseparable.
3. Doppler frequency shift maps directly to angle-of-arrival (angle-of-departure) when the RX (TX) is mobile [14] and so does not provide additional information for clustering.

References

[1] J. Senic, C. Gentile, P.B. Papazian, et al., "Analysis of E-band Path Loss and Prpagation Mechanisms in the Indoor Environment," *IEE Trans. on Antennas and Propagation*, June 2017.

[2] http://www.ieee802.org/11/Reports/tgay_update.htm

[3] P. Kyosti, J. Meinila, L. Hentila, et al., "WINNER II Channel Models," Technical Report EC FP6, Sept. 2007.

[4] L. Liu, C. Oestges, J. Poutanen, et al., "The COST 2100 MIMO Channel Model," *IEEE Wireless Communications*, vol. 19, no. 6, pp. 92-99, 2012.

[5] 5G Special Interest Group homepage: http://www.5gworkshops.com/5GCM.html

[6] METIS II Project homepage: https://metis-ii.5g-ppp.eu/

[7] A. Maltsev, A. Pudeyev, I. Karls, et al., "Quasi-deterministic Approach to mmWave Channel Modeling in a Non-stationary Environment," *IEEE GLOBECOM*, Dec. 2014.

[8] mm MAGIC Project homepage: https://5g-mmmagic.eu/

[9] R. Sun, P.B. Papazian, J. Senic, et al., "Design and Calibration of a Double-directional 60 GHz Channel Sounder for Multipath Component Tracking," *IEEE EuCAP*, March 2017.

[10] P. B. Papazian, C. Gentile, K.A. Remley, et al., "A Radio Channel Sounder for Mobile Millimeter-Wave Communications: System Implementation and Measurement Assessment," *IEEE Trans. on Microwave Theory and Techniques*, vol. 64, no. 9, pp. 2924-2932, Aug. 2016.

[11] M. Ester, H. P. Kriegel, J. Sander, et al., "A Density-based Algorithm for Discovering Clusters in Large Spatial Databases with Noise," *ACM KDD*, Aug. 1996.

[12] W. S. Cleveland and S. J. Devlin, "Locally Weighted Regression: An Approach to Regression Analysi by Local Fitting," Journal of the American Statistical Association, vol. 83, pp. 596-610, 1988.

[13] N. Czink, P. Cera, J. Salo, et al., "A Framework for Automatic Clustering of Parametric MIMO Channel Data Including Path Powers," *IEEE Vehicular Tech. Conf., Fall*, Sept. 2006.

[14] J. Wang, C. Gentile, P.B. Papazian, et al., "Quasi-Deterministic Model for Doppler Spread in Millimeter-wave Commmunication Systems," *IEEE Antennas and Wireless Propagation Letters*, May 2017.